J Solution Chem (2009) 38: 893–905
DOI 10.1007/s10953-009-9417-0

Explosivity Conditions of Aqueous Solutions

R. Thiéry · L. Mercury

Received: 31 December 2008 / Accepted: 3 March 2009 / Published online: 7 May 2009

Abstract This paper focuses on the conditions for explosive boiling and gas exsolution of aqueous solutions from a thermodynamic point of view. Indeed, the kinetic nature of these processes, hence their explosivity, can be assessed by considering their relation with the spinodal curve of these liquids. First, the concepts of mechanical and diffusion spinodals are briefly described, which allows us to introduce the notions of superspinodal (explosive) transformations and subspinodal (non-explosive) ones. Then, a quantitative study of spinodal curves is attempted for the binary systems H_2O–CO_2 and H_2O–NaCl using equations of state having a strong physical basis. It is shown that dissolved gaseous components and electrolytes have an antagonist effect: dissolved volatiles (like CO_2) tend to shift the superspinodal region towards lower temperatures, whereas electrolytes (like NaCl) tend to extend the metastable field towards higher temperatures.

Keywords Metastability · Equation of state · Spinodal · Carbon dioxide · Sodium chloride · Supersaturation

1 Introduction

Water is the main natural explosive agent on the Earth. This fact is well testified by all forms of volcanic and hydrothermal explosive manifestations, which are produced by a sudden and rapid vaporization of water and other dissolved volatiles from a condensed state, either from aqueous solutions or from supersaturated magmas [1]. This paper is mainly devoted to the first case and tackles the explosivity conditions for aqueous solutions. The traditional approach to such problems is to use kinetic theories for bubble nucleation and growth, and this

R. Thiéry (✉)
Laboratoire Magmas et Volcans, UMR 6524, CNRS/Clermont Université/OPGC, 5 rue Kessler, 63038 Clermont-Ferrand Cedex, France
e-mail: r.thiery@opgc.univ-bpclermont.fr

L. Mercury
Institut des Sciences de la Terre d'Orléans, UMR 6113, CNRS/Universités Orléans-Tours, 1A rue de la Férollerie, 45071 Orléans Cedex, France

topic has already been the subject of an abundant literature (see [2, 3]). An alternative and complementary method is applied here by following a phenomenological thermodynamic point of view. Indeed, an explosive situation is generated when a boiling transformation perturbs a liquid up to or through a thermodynamic frontier, i.e., a spinodal, delimiting a thermodynamically forbidden and unstable region of the phase diagram of the system. First, the theoretical grounds of this paradigm are briefly justified, and it will be shown how boiling and gas exsolution can be differentiated, depending upon the process conditions, either in explosive transformations or non-explosive ones. Then, these concepts will be applied to two important types of aqueous solutions, the H_2O–CO_2 and the H_2O–NaCl systems, with the help of thermodynamic models founded on a solid physical basis. This thermodynamic modeling will permit us to decipher the thermodynamic factors controlling the explosivity of boiling and gas exsolution of aqueous solutions.

2 Explosivity: Theoretical Concepts

An explosion is always the response of a system to a physico-chemical perturbation, which has shifted it into a transient and unstable state. The system reacts by a physical or chemical transformation, accompanied by a net volume increase, thus exerting mechanical work on its surroundings. The damages are mainly the result of elevated kinetic rates, hence to the high rate of energy release characterizing the power or yield of the explosion.

2.1 What Defines the Instability of a System?

The stability of a system is ruled by the Second Law of thermodynamics. A first consequence, which can be derived from this principle, is the mechanical stability criterion:

$$\left(\frac{\partial p}{\partial v}\right)_T \leq 0 \tag{1}$$

which states that at a constant temperature T, an increase of the volume v of a closed system must result in a decrease of the internal pressure p. The equality $(\partial p/\partial v)_T = 0$ indicates a limiting state between the metastability and the instability fields, defining the so-called mechanical spinodal state. Another consequence of the Second Law, which can be derived for fluid mixtures [4], is the diffusion stability criteria, which requires spontaneous diffusion (i.e., in the absence of any external force) of species from concentrated regions to less concentrated ones. Mathematically, this statement is formulated by:

$$\left(\frac{\partial^2 G}{\partial x_i^2}\right)_{T,p,x_j} \geq 0 \tag{2}$$

where G is the Gibbs energy and the x_i's refer to mole fractions. Again, the limiting case $(\partial^2 G/\partial x_i^2)_{T,p,x_j} = 0$ corresponds to a frontier of the instability field and defines the so-called diffusion spinodal state [4, 5]. Both mechanical and diffusion stability criteria are features of the intrinsic stability of a fluid with respect to any density or concentration fluctuations, but are not sufficient to fully characterize the stability of a fluid against the formation of a new phase. This latter aspect can only be assessed by fluid phase equilibria calculations. As a result, the phase diagram (Fig. 1) of any system is subdivided into three domain types: (1) an instability region where at least one stability criteria is violated; (2) the stability

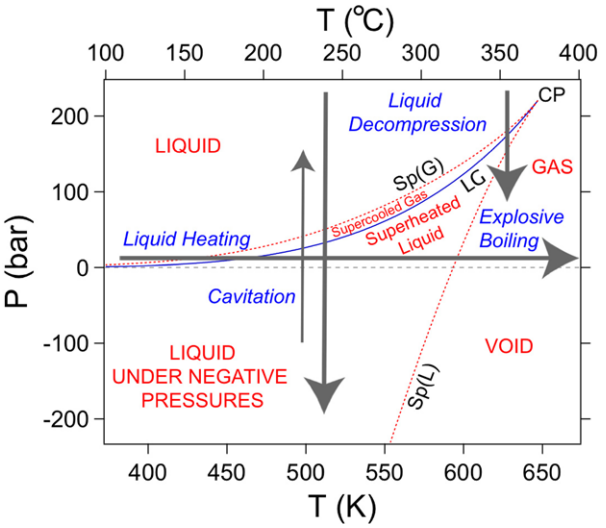

Fig. 1 Pressure–temperature diagram illustrating different perturbation processes of liquid water, and their relations with the stable, metastable and unstable fields of H_2O. *Solid line,* the saturation curve (LG); *dotted lines*, the liquid spinodal curve Sp(L) and the gas spinodal curve Sp(G)

region; and (3) the metastability fields, where all stability criteria are fulfilled. However, in the metastability region, the fluid phase does not correspond to the most stable state of the system, and the demixing of a new phase is expected to occur, lowering the Gibbs energy of the system, as predicted by the Second Law of thermodynamics. The lifetime of a metastable fluid is highly variable [6] and depends on kinetic and other external parameters.

Figure 1 shows these stability, metastability and instability fields for pure water, as calculated by the Wagner and Pruss equation of state [7], in a pressure–temperature plot. Only the mechanical stability criterion is relevant to this one-component system. Limiting stability conditions are encountered along the liquid spinodal curve, denoted by Sp(L), and along the gas spinodal curve, denoted by Sp(G). Both spinodal curves meet at the critical point CP of the liquid–gas (LG) saturation curve (also called binodal). The gas spinodal curve indicates the theoretical extreme conditions that can be attained by a metastable gas (referred to as a supercooled gas). In other words, the liquid spinodal curve marks the furthest theoretical conditions reachable by a metastable liquid (or superheated liquid) before it becomes demixed into a liquid–gas mixture. Figure 1 also depicts the two main physical processes that can trigger the boiling of a liquid in a one-component system: these conditions are (1) isobaric boiling and (2) adiabatic decompression (which can be approximated as a quasi-isothermal process for a liquid [1]).

2.2 Which Features Determine the Explosivity of a Physical Transformation?

In practice, spinodal states of liquid–gas transitions cannot be studied experimentally with the notable exception of the critical point, which is where both gas and liquid spinodal points also touch the stable region. The lifetime of a metastable fluid decreases drastically as the spinodal curve is approached [6], due to the decreasing work for vapor formation (= decreasing liquid–vapor surface tension). Thus, only rapid processes, e.g., a very quick heating step or a sudden decompression (Fig. 1), are able to transport a liquid up to the spinodal conditions. Energetic barriers for nucleation then decrease to the same order of magnitude as molecular fluctuations. Thus, bubble nucleation becomes active and spontaneous mechanisms, in contrast to the cases of weak supersaturation or small degrees of superheating

where nucleation of bubbles are known to be slow processes, which must be activated to occur. Kiselev [8], and Kiselev and Ely [9] have calculated precisely the pressure–temperature conditions for this change of the nucleation regime of water, introducing the notion of a kinetic spinodal. This curve mimics the trend of the thermodynamic liquid spinodal curve (but is shifted to lower temperatures in a pressure-temperature plot). Moreover, experimental studies of liquid–liquid demixing in alloys or polymers, as well numerical simulations, have demonstrated that the usual matter separation for nucleation-phase growth is replaced by the faster and more efficient process of spinodal decomposition [2, 10] in the instability domain (which is when the liquid crosses the thermodynamic spinodal). Hence, the approach of a superheated liquid to spinodal conditions is synonymous with explosive vaporization.

This paradigm has been validated by the analysis of numerous explosions in industry. One type of explosion is caused by the sudden depressurization of liquids. In the specialized literature, this phenomenon is commonly referred to as a BLEVE [11–16] (acronym for a Boiling Liquid Expansion Vapor Explosion). Another type of explosion is produced by the fortuitous contact of a liquid with a hot body at the origin of FCI (Fuel Coolant Interactions) or MFCI (Molten Fuel Coolant Interactions) explosions [17–19]. In each of these categories (BLEVE and FCI), the explosions are interpreted as resulting mainly from the destabilization of a fluid at near-spinodal conditions. A schematic illustration is given in Fig. 2 for the case of sudden liquid decompression. The initial state is a liquid at some temperature T_0 and pressure p_0, well above the external pressure. The vessel is opened suddenly, triggering a fast and adiabatic decompression of the liquid. The following analysis depends upon the initial temperature T_0.

In the first case (left part of Fig. 2), the depressurization leads only to some bubble nucleations and produces moderate foaming at the liquid surface. In the second case (right part of Fig. 2), relevant to a BLEVE explosion, the opening of the tank is accompanied by a shock wave and possibly by its failure resulting in the emission of projectiles. The boiling proceeds here by active spontaneous bubble nucleation (when the liquid pressure drops below the kinetic spinodal), or conceivably by spinodal decomposition (close to or even beyond the thermodynamic spinodal) in the case of very high depressurization rates. The thermodynamic interpretation [17] of these two different evolutions is given in the bottom part of Fig. 2, and involves the spinodal temperature T_{sp} at ambient pressure ($T_{sp} = 320.45\,°C = 593.6$ K for pure water at one bar, as calculated with the Wagner and Pruss equation of state [1, 7]). In the first case, the adiabatic decompression occurs at a temperature below T_{sp}; the depressurization path does not cut the liquid spinodal curve Sp(L) and no explosion occurs. In the second case, the liquid spinodal curve Sp(L) is intersected by the adiabatic depressurization path, and the decompression occurs at a temperature above T_{sp}, triggering a large-scale explosion. Therefore, we suggest introducing the terms subspinodal for non-explosive transformations, and superspinodal for the case of explosive ones.

Note that this interpretation should not be applied too restrictively. Experience shows that some explosive boilings can occur at temperatures below T_{sp} [16]. The spinodal temperature T_{sp} is a purely thermodynamic concept, and the temperature T_{hn} of homogeneous nucleation [1, 2] ($T_{hn} = 304\,°C$, 577 K at one bar for pure water), which is a kinetic parameter, could be more appropriate. Moreover, depending upon the circumstances, decompression under subspinodal conditions does not always trigger boiling, and the solution then becomes supersaturated. In the case of a transient decompression in a confined system, cavitation (Fig. 1) can take place [1].

Nevertheless, thermodynamics provides us with a simple concept which can help us to analyze the possible evolution, explosive or not, of a boiling or gas exsolution process. However, while the liquid spinodal curve of water is presumably well known, at least in its

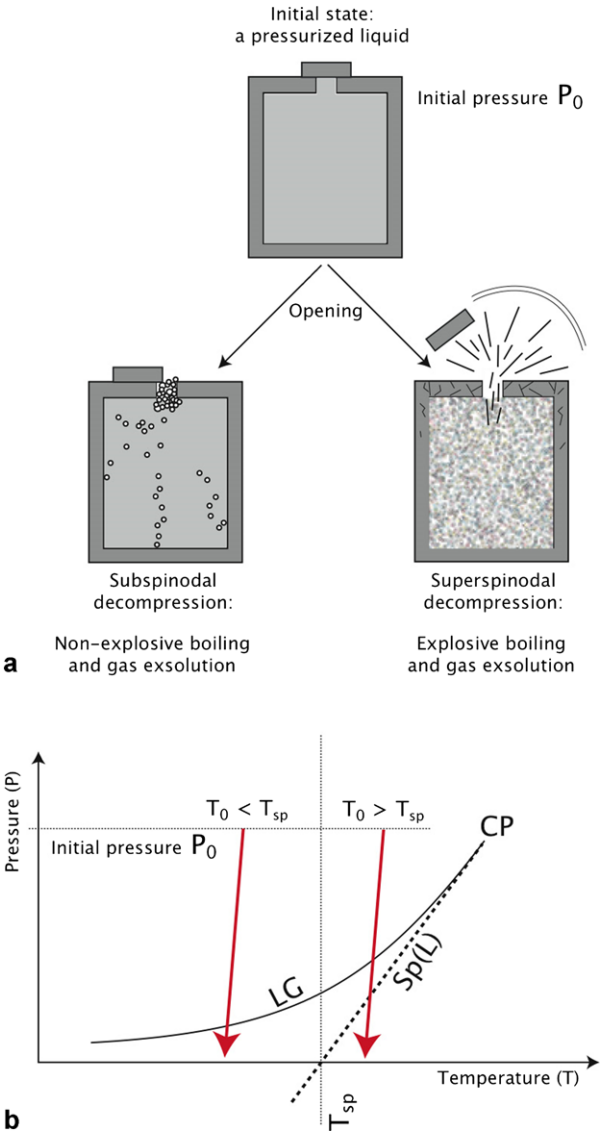

Fig. 2 **a** Schematic illustration of a subspinodal (*left*) and a superspinodal (*right*) decompression. **b** Thermodynamic interpretation of the depressurization explosivity in a pressure–temperature diagram

high-temperature part [5], the topology of spinodal curves of aqueous solutions is poorly known. The purpose of the next two sections is to fill in this gap for CO_2 and NaCl aqueous solutions.

3 The H_2O–CO_2 System

The representation of spinodals is a highly demanding task for an equation of state, as calculations are done beyond the range they were fitting with experimental data. As a consequence, this analysis requires a model with good extrapolation capabilities. A corollary is that we must restrict ourselves to equations of state with a good physical basis, and which

do not rely on ill-founded empirical correlations. Moreover, the H_2O–CO_2 system involves rather complex molecular interactions, which are not easy to describe rigorously [20, 21]. Indeed, H_2O is a strongly dipolar molecule, which associates with neighboring water molecules through hydrogen bounds, whereas CO_2 is a quadrupolar molecule. A first approximation is based on van der Waals-like equations of state (the so-called cubic equations of state), but which incorporate into their attractive a parameter the effects of hydrogen bounds, dipole-dipole and dipole-quadrupole interactions. A first attempt was made with the Daridon equation of state [22], which is able to represent quantitatively the solubility curves of systems like H_2O–CH_4, H_2O–hydrocarbons and H_2O–CO_2 [22, 23]. However, preliminary tests forced us to reject this equation of state, as its good description of immiscibility curves has been forced by using complex empirical expressions for the binary interaction parameters k_{ij} between H_2O and CO_2. This leads to a strong deterioration of its extrapolation abilities (in particular, it fails to correctly represent the H_2O–CO_2 critical curve). Therefore, we chose another cubic equation of state, the Peng-Robinson-Stryjek-Vera (PRSV) equation of state [24–26], which gives good results for mixtures of polar and nonpolar components [27]. A quadratic mixing rule with a zero binary interaction parameter between H_2O and CO_2 has been selected to describe the mixing properties of water and carbon dioxide. Therefore, results given here have to be considered as semi-quantitative. Nevertheless, they should give a reasonable idea of the topology of spinodal curves in water–gas systems. All calculations (thermodynamic properties, binodals, spinodals, critical curves) have been made with the help of the LOTHER library [20, 21, 28] for fluid phase equilibria modeling.

Figure 3a gives solubility curves and spinodals calculated with the PRSV equation of state at 323 K (≈50 °C) in a pressure–mole fraction of CO_2 diagram. For comparison, the solubility curve L(G) of CO_2 in water, calculated with the more accurate model of Duan and Sun [29], is also drawn. Thus, one can observe that the PRSV equation of state underestimates the CO_2 solubility in water, but this was not our first priority. The mechanical spinodal curves for the liquid, denoted as mSp(L), and for the gas, denoted as mSp(G), are plotted along with the diffusion spinodal curves Sp(L) and Sp(G).

The relations between spinodal curves can be observed more clearly on a molar volume versus mole fraction of CO_2 plot (Fig. 3b). Mechanical spinodal curves mSp(L) and mSp(G) meet at a pseudo-critical point (pCP) where the additional constraint is fulfilled [5, 30]:

$$\left(\frac{\partial^2 p}{\partial v^2}\right)_{T,x_j} = 0 \tag{3}$$

The diagram also shows that for the whole composition range, the mechanical instability field (and the pCP) is included in the diffusion instability domain. This result can be generalized and has been demonstrated by Imre and Kraska [5] for different types of mixtures. Thus, for mixtures, the relevant stability criterion is not the mechanical one, but the diffusion one.

Calculations reveal that reversible and adiabatic (i.e., isentropic) liquid decompressions lead to only moderate temperature decreases up to the liquid spinodal curve for pure water [1]. Although sudden liquid depressurizations are highly irreversible transformations, they can also be assumed, to a first approximation, as being nearly isothermal processes before the onset of gas demixing. Thus, isothermal pressure–compositions sections (Figs. 3 and 4) provide useful diagrams to analyze the explosive character of these rapid and strong liquid decompressions.

The projections of the L(G) and Sp(L) isotherms in the p–x_{CO_2} diagram of Fig. 3a are almost vertical and parallel. As a consequence, the depressurization of a CO_2-supersaturated

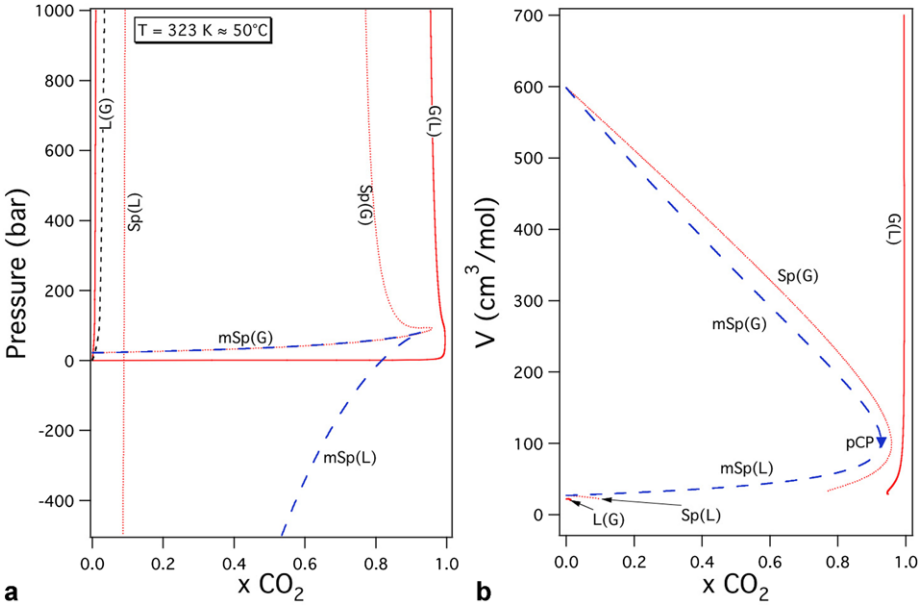

Fig. 3 **a** Pressure–CO_2 mole fraction diagram showing the boundaries of stable, metastable and unstable fields, as calculated with the PRSV equation of state for the H_2O–CO_2 system at 323 K (≈50 °C). *Solid lines*, the solubility curve L(G) of CO_2 in liquid water and the solubility curve G(L) of H_2O in gaseous CO_2; *dotted lines*, the diffusion liquid Sp(L) and gas Sp(G) spinodal curves; *long dashed curves*, the mechanical liquid mSp(L) and gas mSp(G) spinodal curves; *short dashed curve*, solubility curve L(G) calculated with the Duan and Sun model [29]. **b** Molar volume–CO_2 mole fraction diagram illustrating the relations between the diffusion and mechanical metastable fields. *Triangle marker*, the pseudo-critical point (pCP) at 323 K

solution cannot perturb the fluid up to near-spinodal conditions: gas exsolution will always proceed only by moderate bubble nucleations and any decompression process will be sub-spinodal.

Superspinodal depressurizations are possible in the H_2O–CO_2 system at much higher temperatures. An example is given in Fig. 4, where binodal and spinodal curves at 623 K (≈350 °C) are projected in a p–x_{CO_2} section. The four curves L(G), G(L), Sp(L) and Sp(G) join at one critical point CP of the H_2O–CO_2 critical curve. Note that other geometric relations (intersection points, in particular) between spinodals and binodals have no physical meaning, and correspond only to artifacts produced by the projection of the phase diagram onto an isothermal pressure–composition section. Moreover, the L(G) and Sp(L) curves are not spaced evenly. For example, a CO_2 aqueous solution with $x_{CO_2} = 0.04$ at 350 °C is saturated at 220 bar, but is already in a spinodal state at 195 bar. Therefore, any severe decompression of a CO_2-saturated solution should lead to a large scale destabilization at this temperature.

Figure 5 depicts the liquid spinodal curves Sp(L) in a pressure–temperature diagram for fixed CO_2 compositions. The region of negative pressures, which is of interest for describing the capillary properties of aqueous CO_2 solutions [31–33], has also been included. Interestingly, it can be noted that spinodal Sp(L) isopleths present a pressure–temperature trend that looks similar to the liquid spinodal curve of pure water [1, 2, 7, 31, 32]. At low temperatures, the Sp(L) isopleths decrease steeply before reaching a pressure minimum. Then at subcritical temperatures, isopleths are less regularly spaced and sloped, and they meet at the

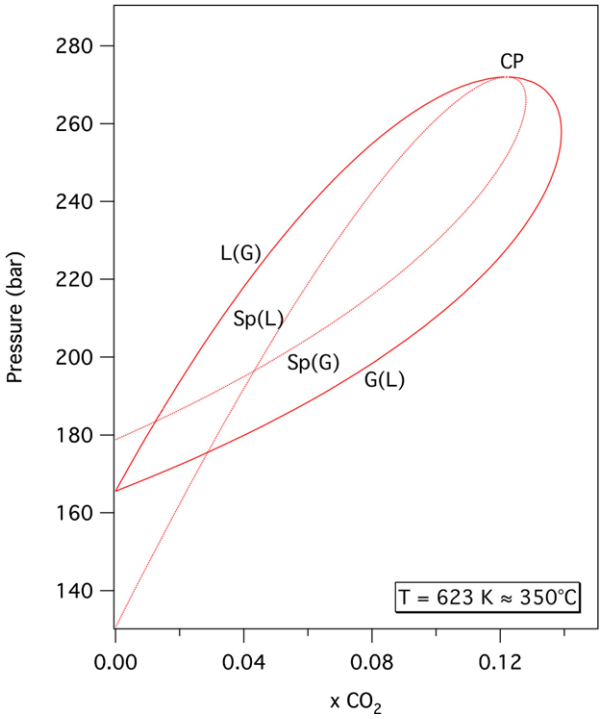

Fig. 4 Two-dimensional projections of the stable, metastable and unstable three-dimensional fields in the H_2O–CO_2 system at 623 K (≈350 °C) onto a pressure–CO_2 mole fraction diagram. The drawn curves do not actually cross each other

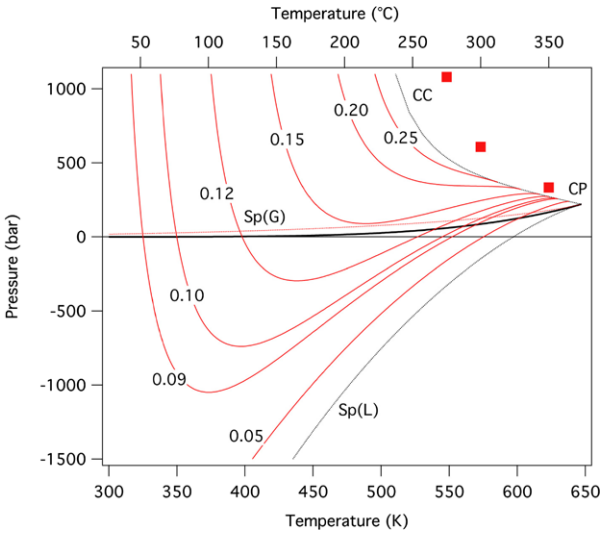

Fig. 5 The liquid spinodal curves in a pressure–temperature diagram for the H_2O–CO_2 system, as calculated with the PRSV equation of state. *Numbers* refer to the mole fraction x_{CO_2} of dissolved CO_2 in the aqueous solution, and *filled squares* are the experimental data of Tödheide and Franck [42] for the H_2O–CO_2 critical curve

H_2O–CO_2 critical curve. Temperature appears as a determining parameter in the explosivity control of CO_2 aqueous solutions. The temperature limit can be estimated as ca. 425 K (≈150 °C), whose value is to be compared with the spinodal temperature T_{sp} of pure water at 1 bar at 320.45 °C [1, 7]. Depressurizations are expected to be subspinodal below this temperature threshold, and superspinodal above it. Therefore, the presence of dissolved volatiles

in aqueous solutions strongly reduces their metastability field towards lower temperatures and accentuates their explosivity potential compared with pure water.

Extrapolation of Henry's law constants when aqueous solutions are under negative pressures led us to conclude that superheated solutions should have an increasing capability to store dissolved gases with respect to stable solutions [31, 32]. This conclusion means that non-saturated media containing capillary solutions (soils, dried zone) could act as an atmospheric CO_2 well. However, what is demonstrated here is that the superheating capability decreases with increasing CO_2 mole fraction. As a consequence, there is certainly a subtle equilibrium between the increasing dissolved gas content in excess of the saturation value, and the superheated state of the solvent which favors it.

4 The H_2O–NaCl System

The same approach as in the preceding section can be applied to study the explosivity conditions of the H_2O–NaCl system. Again, one is faced with the same problem of model selection. The Anderko-Pitzer (AP) equation of state [34] has been chosen here, as it is based on realistic physical hypotheses. It describes the H_2O–NaCl system by means of statistical thermodynamic models [35, 36] developed for dipolar hard spheres. This assumption is reasonable at high temperatures, where NaCl is known to form dipolar ion pairs. However, for this reason, this equation of state is only applicable above 573 K (300 °C). The AP equation of state reproduces quite well the critical curve of H_2O–NaCl up to 1100 K [28, 34], and this is another important selection criteria in the search for a good model for spinodal calculations.

Figure 6 displays a p–x_{NaCl} diagram depicting binodal and spinodal isotherms at 623 K (350 °C). The equation of state reproduces well the tabulated data of Bischoff [37] for the solubility curves L(G) and G(L). The pressures of the diffusion spinodal curves Sp(L) and Sp(G) decrease with increasing x_{NaCl} mole fractions. Note also that the spinodal curves run through the stability field of halite at pressures below 100 bar. Also, other studies (e.g., [31–33]) have already shown that solid–liquid lines are sensitive to the metastable states

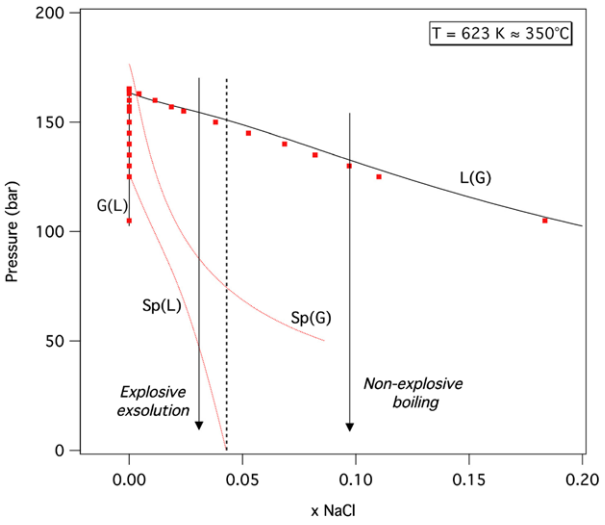

Fig. 6 The stable, metastable and unstable fields in a pressure–NaCl mole fraction diagram for the H_2O–NaCl system at 623 K (≈350 °C), as calculated with the Anderko and Pitzer equation of state [34]. *Solid lines*, the solubility curves L(G) and G(L); *dotted lines*, the spinodals Sp(L) and Sp(G); *squared markers*, experimental data compiled by Bischoff [37]

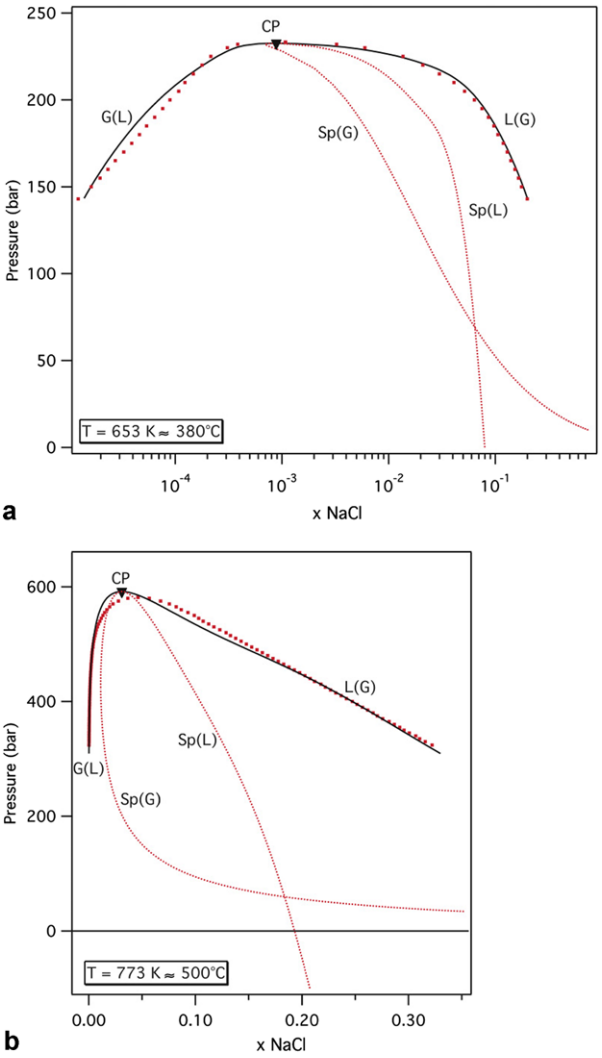

Fig. 7 Pressure–NaCl mole fractions diagrams of the H_2O–NaCl system, as calculated with the Anderko and Pitzer equation of state [34]: **a**, at 653 K (≈380 °C); **b**, at 773 K (≈500 °C)

inside the system, which should result in subtle interplays between all of these effects in geochemical contexts.

In terms of LV partitioning, the H_2O–NaCl system presents dual behavior concerning its stability during rapid depressurization. For x_{NaCl} values between 0 and 0.04, a decompression path down to the atmospheric pressure will intersect the liquid spinodal curve Sp(L). This will trigger an explosive exsolution of H_2O from the brine, featuring a superspinodal process. Differently, for higher x_{NaCl} values, the spinodal curve Sp(L) runs to negative pressures, and any severe depressurization can only generate non-explosive boiling of the concentrated brines, characterizing a subspinodal transformation.

Two other portraits of the metastability fields of the H_2O–NaCl system are given in the p–x_{NaCl} diagrams of Fig. 7a (at 380 °C) and Fig. 7b (at 500 °C), i.e., at temperatures above the critical point of H_2O. Now, both spinodal Sp(L) and Sp(G) isotherms join at a critical point (CP). Another intersection point can be observed at lower pressures, but beware, this

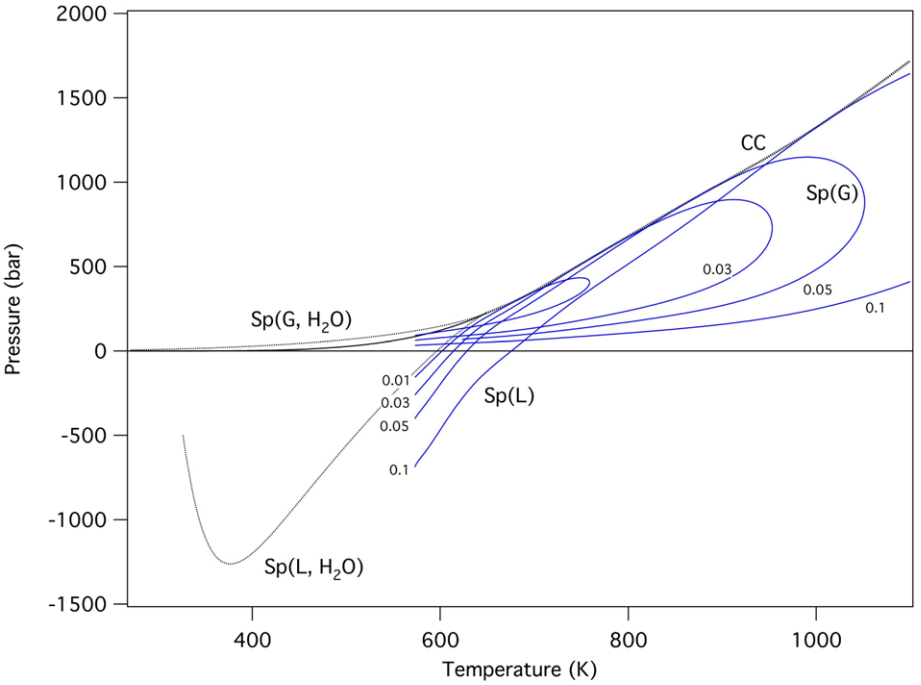

Fig. 8 Stability fields, calculated with the Anderko and Pitzer equation of state [34], of the H_2O–NaCl system in a pressure-temperature diagram. *Solid lines*: the saturation curve (LG) of pure water and the spinodal isopleths of H_2O–NaCl fluids (*numbers* refer to the mole fractions of NaCl); *dotted lines*: the liquid spinodal curve Sp(L, H_2O) and gas spinodal curve Sp(G, H_2O) of pure water

is only an artifact generated by the projection of spinodal isotherms onto the p–x_{NaCl} planes. Again, H_2O–NaCl brines present the same contrasting behavior when they are submitted to a sudden depressurization. Below some x_{NaCl} threshold value (e.g., for $x_{NaCl} < 0.08$ at 380 °C and $x_{NaCl} < 0.19$ at 500 °C), fast decompressions will result in superspinodal vaporizations. Thus, subspinodal boilings occur for only rather concentrated brines at these elevated temperatures. Note also that the metastability field of supercooled vapors (i.e., between the G(L) and Sp(G) curves) extends over a non-negligible range of pressures and NaCl compositions.

Figure 8 illustrates the metastability fields of the H_2O–NaCl system in a p–T diagram by means of a series of spinodal isopleths calculated, respectively, for $x_{NaCl} = 0.01$, 0.03, 0.05 and 0.1. Each isopleth defines a loop, which is tangential to one point of the H_2O–NaCl critical curve. At this critical point, the nature of the isopleth changes from a liquid spinodal Sp(L) to a gas spinodal Sp(G). The diagram shows clearly that the addition of NaCl progressively shifts the liquid spinodal curve Sp(L) to higher temperatures: e.g., the spinodal temperature at 1 bar increases from 320.45 °C at $x_{NaCl} = 0$ to 403 °C at $x_{NaCl} = 0.1$ (i.e., 26.5 NaCl wt-%, but within the stability field of halite). Hence, high concentrations of electrolytes favor metastability for aqueous solutions. This conclusion is in agreement with experimental data for synthetic fluid inclusions reported by Shmulovich et al. [38], and with the observed behavior of natural hydrothermal systems involving the circulation of brines [39].

5 Conclusions

Spinodals represent an appealing concept, which allows us to link the kinetics of physical transformations to the corresponding thermodynamic properties of the system. Explosive vaporizations can be identified as processes that perturb a liquid around near-spinodal singularities. This simple criterion, which is commonly applied by safety engineering in the industrial domain, has been generalized here to the case of aqueous solutions. The present modeling study shows the antagonist effects of dissolved volatiles and electrolytes (at least, for all components that behave like CO_2 and NaCl): gaseous species tend to shift the explosivity conditions to lower temperatures, whereas dissolved salts tend to displace spinodal conditions to higher temperatures. This work can give useful indications to constrain the modeling of hydrothermal, phreatic and phreato-magmatic eruptions (for instance, the Lake Nyos disaster, which is explained by some models to result from the explosive CO_2 exsolution of dormant supersaturated water [40, 41]).

Acknowledgements This work has been financially supported by the Agence Nationale de la Recherche (ANR) for the project SURCHAUF-JC05-48942. Two anonymous reviewers helped us to improve the quality of the initial manuscript. Donald Palmer is also acknowledged both for the invitation to submit a paper and for the editorial handling.

References

1. Thiéry, R., Mercury, L.: Explosive properties of water in volcanic and hydrothermal systems. J. Geophys. Res. (2009). doi:10.1029/2008JB005742
2. Debenedetti, P.: Metastable Liquids. Princeton University Press, Princeton (1996)
3. Lasaga, A.: Kinetic Theory in the Earth Sciences. Princeton University Press, Princeton (1998)
4. Rowlinson, J., Swinton, F.: Liquid and Liquid Mixtures, 3rd edn. Butterworth Scientific, London (1982)
5. Imre, A., Kraska, T.: Stability limits in binary fluid mixtures. J. Chem. Phys. **122**, 1–8 (2005)
6. El Mekki, M., Ramboz, C., Perdereau, L., Shmulovich, K.I., Mercury, L.: Lifetime of superheated water in a micrometric fluid inclusion. In: Rzoska, S.J., Mazur, V. (eds.) Metastable Systems under Pressure: Platform for New Technological and Environmental Applications. Springer, Dordrecht (2009)
7. Wagner, W., Pruss, A.: The IAPWS formulation 1995 for the thermodynamic properties of ordinary water substance for general and scientific use. J. Phys. Chem. Ref. Data **31**, 387–535 (2002)
8. Kiselev, S.: Kinetic boundary of metastable states in superheated and stretched liquids. Physica A **269**, 252–268 (1999)
9. Kiselev, S., Ely, J.: Curvature effect on the physical boundary of metastable states in liquids. Physica A **299**, 357–370 (2001)
10. Debenedetti, P.: Phase separation by nucleation and by spinodal decomposition: fundamentals. In: Kiran, E., Debenedetti, P., Peters, C.C. (eds.) Supercritical Fluids: Fundamentals for Application, pp. 123–166. Kluwer Academic, Dordrecht (2000)
11. Abbasi, T., Abbasi, S.: The boiling liquid expanding vapour explosion (BLEVE): mechanism, consequence assessment, management. J. Hazard. Mater. **141**, 480–519 (2007)
12. Casal, J., Salla, J.: Using liquid superheating for a quick estimation of overpressure in BLEVEs and similar explosions. J. Hazard. Mater. A **137**, 1321–1327 (2006)
13. Planas-Cuchi, E., Salla, J., Casal, J.: Calculating overpressure from BLEVE explosions. J. Loss Prevent. Process Ind. **17**, 431–436 (2004)
14. Pinhasi, G., Ullmann, A., Dayan, A.: 1D plane numerical model for boiling liquid vapor explosion (BLEVE). Int. J. Heat Mass Transf. **50**, 4780–4795 (2007)
15. Salla, J., Demichela, M., Casal, J.: BLEVE: a new approach to the superheat limit temperature. J. Loss Prevent. Process Ind. **19**, 690–700 (2006)
16. Reid, R.C.: Possible mechanism for pressurized-liquid tank explosions or BLEVE's. Science **203**, 1263–1265 (1979)
17. Reid, R.C.: Superheated liquids. Am. Sci. **64**, 146–156 (1976)
18. Reid, R.C.: Rapid phase transitions from liquid to vapor. Adv. Chem. Eng. **12**, 105–208 (1983)
19. Corradini, M.L., Kim, B.J., Oh, M.D.: Vapor explosions in light water reactors: a review of theory and modeling. Prog. Nucl. Energy **22**(1), 1–117 (1988)

20. Perfetti, E., Thiéry, R., Dubessy, J.: Equation of state taking into account dipolar interactions and association by hydrogen bonding. I—Application to pure water and hydrogen sulfide. Chem. Geol. **251**, 58–66 (2008)
21. Perfetti, E., Thiéry, R., Dubessy, J.: Equation of state taking into account dipolar interactions and association by hydrogen bonding: II—Modelling liquid-vapour equilibria in the H_2O–H_2S, H_2O–CH_4 and H_2O–CO_2 systems. Chem. Geol. **251**, 50–57 (2008)
22. Daridon, J., Lagourette, B., Saint-Guirons, H., Xans, P.: A cubic equation of state model for phase equilibrium calculation of alkane + carbon dioxide + water using a group contribution k_{ij}. Fluid Phase Equil. **91**, 31–54 (1993)
23. Thiéry, R.: Thermodynamic modeling of aqueous-CH_4 bearing fluid inclusions trapped in hydrocarbon-rich environments. Chem. Geol. **227**, 154–164 (2006)
24. Stryjek, R., Vera, J.: An improved Peng-Robinson equation of state with new mixing rules for strongly non ideal mixtures. Can. J. Chem. Eng. **64**, 334–340 (1986)
25. Stryjek, R., Vera, J.: PRSV2: a cubic equation of state for accurate vapour-liquid equilibrium calculations. Can. J. Chem. Eng. **64**, 820–826 (1986)
26. Stryjek, R., Vera, J.: Vapour-liquid equilibria of hydrochloric acid and solutions with the PRSV equation of state. Fluid Phase Equil. **25**, 279–290 (1986)
27. Duan, Z., Hu, J.: A new cubic equation of state and its applications to the modeling of vapor-liquid equilibria and volumetric properties of natural fluids. Geochim. Cosmochim. Acta **14**, 2997–3009 (2004)
28. Thiéry, R.: A new object-oriented library for calculating high-order multivariable derivatives and thermodynamic properties of fluids with equations of state. Comput. Geosci. **22**, 801–815 (1996)
29. Duan, Z., Sun, R.: An improved model calculating CO_2 solubility in pure water and aqueous NaCl solutions from 273 to 533 K and from 0 to 2000 bar. Chem. Geol. **193**, 257–271 (2003)
30. Asselineau, L., Bogdanic, G., Vidal, J.: A versatile algorithm for calculating vapour-liquid equilibria. Fluid Phase Equil. **3**, 273–290 (1979)
31. Mercury, L., Azaroual, M., Zeyen, H., Tardy, Y.: Thermodynamic properties of solutions in metastable systems under negative or positive pressures. Geochim. Cosmochim. Acta **67**, 1769–1785 (2003)
32. Mercury, L., Pinti, D.L., Zeyen, H.: The effect of the negative pressure of capillary water on atmospheric noble gas solubility in ground water and palaeotemperature reconstruction. Earth Planet. Sci. Lett. **223**, 147–161 (2004)
33. Pettenati, M., Mercury, L., Azaroual, M.: Capillary geochemistry in non-saturated zone of soils. Water content and geochemical signatures. Appl. Geochem. **23**, 3799–3818 (2008)
34. Anderko, A., Pitzer, K.: Equation-of-state representation of phase equilibria and volumetric properties of the system NaCl–H_2O above 573 K. Geochim. Cosmochim. Acta **57**, 1657–1680 (1993)
35. Boublik, T.: Hard sphere equation of state. J. Chem. Phys. **53**, 471–472 (1970)
36. Stell, G., Rasaiah, J., Narang, H.: Thermodynamic perturbation theory for simple polar fluids. J. Mol. Phys. **23**, 393–406 (1972)
37. Bischoff, J.: Densities of liquids and vapors in boiling NaCl–H_2O solutions: a PVTX summary from 300 to 500 °C. Am. J. Sci. **291**, 369–381 (1991)
38. Shmulovich, K., Mercury, L., Thiéry, R., Ramboz, C., El Mekki, M.: Superheating ability of water and aqueous solutions. Experiments and geochemical consequences. Geochim. Cosmochim. Acta **73**(9), 2457–2470 (2009)
39. Orphanidis, E.: Conditions physico-chimiques de précipitation de la barytine épigénétique dans le bassin sud-ouest de la fosse Atlantis II (Mer Rouge): données des inclusions fluides et approche expérimentale. Implications pour le dépôt des métaux de base et métaux précieux. Thèse Université d'Orléans, 180 pp. (1995)
40. Rice, A.: Rollover in volcanic crater lakes: a possible cause for Lake Nyos type disasters. J. Volcan. Geotherm. Res. **97**, 233–239 (2000)
41. Schuiling, R.D., Cathcart, R.B., Badescu, V.: Asteroid impact in the Black Sea; a black scenario. In: Rzoska, S.J., Mazur, V. (eds.) Soft Matter under Exogenic Impacts. NATO Science Series II, vol. 242, pp. 2–8. Springer, Dordrecht (2007)
42. Tödheide, K., Franck, E.U.: Das Zweiphasengebiet und die kritische Kurve im System Kohlendioxid-Wasser bis zu Drucken von 3500 bar. Z. Phys. Chem. **37**, 387–401 (1963)